This article has been accepted for inclusion in a future issue of this journal. Content is final as presented, with the exception of pagination.

New Optimized Spectral Indices for Identifying and Monitoring Winter Wheat Diseases

Wenjiang Huang, Qingsong Guan, Juhua Luo, Jingcheng Zhang, Jinling Zhao, Dong Liang, Linsheng Huang, and Dongyan Zhang

***Abstract*—The vegetation indices from hyperspectral data have been shown to be effective for indirect monitoring of plant diseases. However, a limitation of these indices is that they cannot distinguish different diseases on crops. We aimed to develop new spectral indices (NSIs) that would be useful for identifying different diseases on crops. Three different pests (powdery mildew, yellow rust, and aphids) in winter wheat were used in this study. The new optimized spectral indices were derived from a weighted combination of a single band and a normalized wavelength difference of two bands. The most and least relevant wavelengths for different diseases were first extracted from leaf spectral data using the RELIEF-F algorithm. Reflectance of a single band extracted from the most relevant wavelengths and the normalized wavelength difference from all possible combinations of the most and least relevant wavelengths were used to form the optimized spectral indices. The classification accuracies of these new indices for healthy leaves and leaves infected with powdery mildew, yellow rust, and aphids were 86.5%, 85.2%, 91.6%, and 93.5%, respectively. We also applied these NSIs for nonimaging canopy data of winter wheat, and the classification results of different diseases were promising. For the leaf scale, the powdery mildew-index (PMI) correlated well with the disease index (DI), supporting the use of the PMI to invert the severity of powdery mildew. For the canopy scale, the detection of the severity of yellow rust using the yellow rust-index (YRI) showed a high coefficient of determination ($R^{2=}0.86$) between the estimated DI and its observations, suggesting that the NSIs may improve disease detection in precision agriculture application.**

***Index Terms*—Aphids, canopy reflectance, hyperspectrum, new spectral indices (NSIs), powdery mildew, winter wheat, yellow rust.**

I. Introduction

WINTER wheat (*Triticumaestivum* L.) is one of the most prevalent crops in China. Many diseases could threaten winter wheat: stripe rust, powdery mildew, aphids, etc. When environmental conditions are favorable, an outbreak of these diseases can spread rapidly, resulting in significant loss of yield and quality [1]. Each disease has its own characteristics and, consequently, requires corresponding measures. Therefore, developing technologies for accurately monitoring and identifying the occurrence of diseases is extremely important in agricultural management.

Detecting and predicting the occurrence of diseases are mainly based on meteorological data, such as temperature and relative humidity, which is acquired with plot-level measurements without spatial distribution information [2]. Fortunately, remote sensing technology provides a way to possibly detect crop diseases at the regional scale. Several advancements have been made to monitor crop diseases, including X-ray, ultrasound, and multispectral and hyperspectral technologies. Among these technologies, the hyperspectral method has several advantages for detecting and monitoring diseases over a vast area [3]. In optical remote sensing, the wavelength range mainly focuses on ultraviolet (200–400 nm), visible (400–800 nm), and shortwave infrared (800–2500 nm) bands. Depending on the application area and aim, a few subregions of the spectrum have recently attracted scholarly interest. By analyzing the leaf spectral of wheat with fusarium head bligh, Delwiche and Kim [4] found that the disease can cause relatively strong spectral responses at 550, 568, 605, 623, 660, 697, 715, and 733 nm. Huang *et al.* [5] studied the spectral characteristics of wheat with yellow rust and identified sensitive bands at 630–687 nm, 740–890 nm, and 976–1350 nm. Based on these findings, the authors used the photochemical reflectance index (PRI) and successfully monitored disease croplands [6]. Rumpf *et al.* [7] detected beet diseases in their earliest stages using a high-precision recognition model based on a support vector machine (SVM) and a spectral index. Mirik *et al.* [8] used airborne hyperspectral imagery and the SVM classifier to effectively identify noxious weeds. Combining independent component analysis and principal component analysis, Muhammed [9] achieved good results in a study on wheat with tan-spot disease.

Several current vegetation indices have been proven effective for indirect monitoring of plant diseases. However, these indices have been limited in their sensitivity to certain plant parameters, such as variations in pigment content [10]–[12], canopy architecture [13, 14], and water status [15, 16]. Using these indices to identify a specific disease remains difficult because the unique spectral characteristics of each condition have yet to be clarified. Therefore, new disease-detecting spectral analysis methods and algorithms are particularly needed; these can likely be achieved through a combination of wavelengths.

Manuscript received June 13, 2013; revised November 16, 2013; accepted November 22, 2013. This work was supported in part by the National Natural Science Foundation of China (41325004, 41271412, 41301471), in part by Hundred Talent Program of the Chinese Academy of Sciences of Wenjiang Huang, and in part by Open Research Fund of Key Laboratory of Digital Earth Science (2012LDE003).

W. Huang and Q. Guan are with the Key Laboratory of Digital Earth Science, Institute of Remote Sensing and Digital Earth, Chinese Academy of Sciences, Beijing 100094, China (e-mail: huangwenjiang@gmail.com; guanqs2206@126.com).

Q. Guan, J. Zhao, D. Liang, L. Huang, and D. Zhang are with the Key Laboratory of Intelligent Computing & Signal Processing, Ministry of Education, Anhui University, Hefei 230039, China (e-mail:aling0123@163.com; dliang@ahu.edu.cn; linsheng0808@163.com; hello-lion@hotmail.com).

J. Luo is with the State Key Laboratory of Lake Science and Environment, Nanjing Institute of Geography and Limnology, Chinese Academy of Sciences, Nanjing 210008, China (e-mail: luojuhua@126.com).

J. Zhang is with the Beijing Research Center for Information Technology in Agriculture, Beijing, China (e-mail: zhangjc@nercita.org.cn).

Color versions of one or more of the figures in this paper are available online at http://ieeexplore.ieee.org.

Digital Object Identifier 10.1109/JSTARS.2013.2294961

In this study, leaf spectral reflectance measurements of crop plants infected with powdery mildew, yellow rust, or aphids were used to develop new spectral indices (NSIs). Four NSIs have been proposed to identify healthy, and powdery mildew-, yellow rust-, and aphids-infected plants. To validate the NSIs, canopy spectral data from field spectroscopy were used.

II. Materials and Methods

A. Field Conditions and Pathogen Inoculation

The experiments were conducted at Beijing Xiaotangshan Precision Agriculture Experimental Base in the Changping district, Beijing ($40°10.6'$N, $116°26.3'$E). The average contents of nutrients in topsoil (0–0.30 m depth) were as follows: organic matter 1.42%–1.48%, total nitrogen 0.08%–0.10%, alkali-hydrolysis nitrogen $58.6 - 68.0\ \mathrm{mg} \cdot \mathrm{kg}^{-1}$, available phosphorus $20.1 - 55.4\ \mathrm{mg} \cdot \mathrm{kg}^{-1}$, and rapidly available potassium $117.6 - 129.1\ \mathrm{mg} \cdot \mathrm{kg}^{-1}$.

The cultivars (98–100 and Jingdong 8) of winter wheat that are susceptible to yellow rust and powdery mildew were inoculated with yellow rust and powdery mildew in early April by spore inoculation according to the National Plant Protection Standards [1]. The cultivar Jingong 8 was also inoculated with aphids. During the growing season, wheat aphids (*Sitobion avenae* F.) also occurred throughout the entire experimental field.

B. Leaf Spectral Measurement

An ASD FieldSpec spectrometer (Analytical Spectral Devices, Inc., Boulder, CO, USA) equipped with a Li-Cor 1800-12 integration sphere (Li-Cor, Inc., Lincoln, NE, USA) was used to measure the reflectance and transmittance of the upper faces of the leaves. The spectrometer was fitted with a 25° field-of-view bare fiber-optic cable and operated in the 350–2500 nm spectral range with a sampling interval of 1.4 nm between 350 and 1050 nm, and 2 nm between 1050 and 2500 nm. The spectral resolution was 3 nm for the 350–1000 nm region and 10 nm for the 1000–2500 nm region. In this study, only the spectral region of 400–1000 nm was analyzed. For each sample, measurements were made on five different areas to quantify the small but not negligible within-leaf variability. The scan time required for each sample was about 2 min. The sample was illuminated by a focused beam, and the radiation that was captured by the spectrometer was the average reflected radiation within the Li-Cor 1800-12 integration sphere. The data were collected in the middle of April because the three diseases were in the incidence at that time.

C. Classification of Disease Index

The disease index (DI) is commonly cited to describe the severity of crop diseases. With the leaf scale, the severity of crop diseases is mainly reflected by the extent of bacterial infection on the leaves and the ratio of the lesion to the healthy part of the plant. Thus, visual judgment of the lesion's coverage ratio on the blade indicates the severity of infection on this scale [17], [18]. Before completing leaf spectral and biochemical parameter measurements, photos were taken of each leaf, and the severity of disease was estimated based on the images. The lesion ratio was divided into 10 categories to reduce human error: 3%–10% (DI = 1), 10.1%–20% (DI = 2), 20.1%–30% (DI = 3), 30.1%–40% (DI = 4), 40.1%–50% (DI = 5), 50.1%–60% (DI = 6), 60.1%–70% (DI = 7), 70.1%–80% (DI = 8), 80.1%–90% (DI = 9), and 90.1%–100% (DI = 10) [13].

INPUT: A set of features F, a set of samples X,
a lable function l, a number of iterations $p \in \mathrm{N}$
and a number of neighbors $k \in \mathrm{N}$
OUTPUT: A set of feature weights $\omega = \{\omega(F_1), \cdots, \omega(F_m)\}$
Set $\omega(F_i) := 0\ \forall i \in \{0, \cdots, m\}$
for $i := 1$ *to* p
Pick $x \in X$ at random
Find k nearest hits $A \subseteq X$ and nearest misses $B \subseteq X$
for $j := 1$ *to* m

$$\omega(F_i) := \omega(F_j) - \frac{1}{k}\sum_{a \in A}\left|x_j - a_j\right| + \frac{1}{k}\sum_{b \in B}\left|x_j - b_j\right|$$

end
end
Set $\omega(F_i) := \dfrac{\omega(F_i)}{m}\ \forall i \in \{0, \cdots, m\}$
return $\{\omega(F_1), \cdots, \omega(F_m)\}$

Fig. 1. Pseudo code of the RELIEF-F algorithm for two-class classification.

D. New Spectral Indices

In this study, we proposed NSIs that can quantitatively distinguish between specific plant diseases. Single wavelength responses to different diseases have their own characteristics, especially when the disease is in advanced stage (i.e., severe). However, normalized wavelength differences of two bands are sensitive to changes in the hyperspectral data as a result of yellow rust, powdery mildew, and aphids [19]. Therefore, NSIs that combine a single wavelength and a normalized wavelength difference can effectively identify specific plant diseases [19].

To find the best combination of single wavelength and wavelength difference, the RELIEF-F algorithm [20] was used. The original Relief algorithm [21] was designed to estimate the quality of attributes according to how well their values distinguished between instances within the close proximity of each other. The RELIEF-F algorithm is not limited to two class problems, and it is more robust and can deal with incomplete and noisy data. The two nearest neighbors of a given sample were sought using the RELIEF-F algorithm. Each neighborhood consists of k samples. For a given k, the set of k nearest neighbors of the same class were deemed a "hit" and from a different class were deemed a "miss". The algorithm is shown in pseudo code in Fig. 1 and detailed information on the RELIEF algorithm can be found in Kira and Rendell [21].

For a specific index, the most relevant single wavelength was obtained using the RELIEF-F algorithm, which belonged to the best weighted (20%) wavelengths. A normalized wavelength difference needed two wavelengths: one from the top 10% (i.e., best weighted single wavelengths) and one from the bottom 10% (i.e., worst weighted). All possible combinations were searched until the distance between the two wavelengths was less than

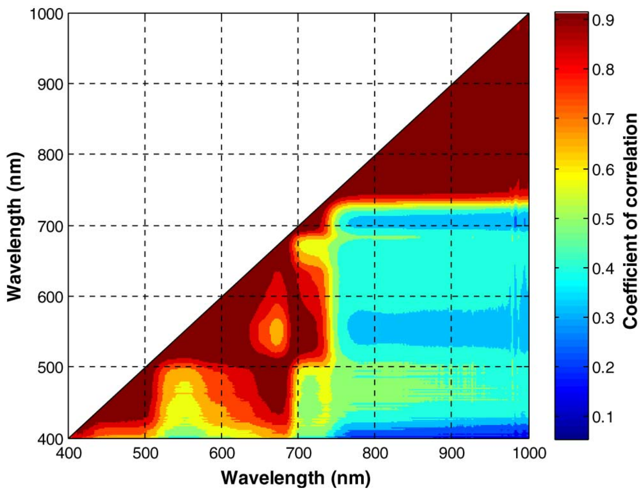

Fig. 2. Contour plot visualizing the correlation of narrow wavelength from 400 to 1000 nm.

50 nm. Finally, the RELIEF-F algorithm was used again to find the best weighted normalized wavelength differences. In addition, we set the possible weights as -0.5 and 0.5 for the single wavelength.

E. Comparison With Common Vegetation Indices

The ability to identify disease with these NSIs was tested and compared with other commonly used vegetation indices from the literature. The primary concern was that these indices should be sensitive to chlorophyll content, canopy architecture, or water status, including the MSR [22], the NDVI [14], the NRI [23], the PRI and PhRI [24], the SIPI [11], the NPCI [25], the ARI [26], the RVSI [27], and the MCARI [28].

F. Application of Datasets

To validate the usefulness of the NSIs, we used canopy spectral data from field spectroscopy and the observed DI of yellow rust in wheat. The datasets were obtained under different measuring conditions and with different sensors.

G. Canopy Spectral Data

The canopy spectral measurements were taken by an ASD FieldSpec Pro spectrometer (Analytical Spectral Devices, Boulder, CO, USA) fitted with 25° field-of-view fiber optics. All canopy spectral measurements were taken from a height of 1.3 m above the ground (the height of the wheat was 90 ± 3 cm at maturity). The spectra were acquired in the 350–2500 nm spectral range at a spectral resolution of 3 nm between 350 and 1050 nm and 10 nm between 1050 and 2500 nm. A $40\ \mathrm{cm} \times 40\ \mathrm{cm}\ \mathrm{BaSO_4}$ calibration panel was used to calculate reflectance. All irradiance measurements were recorded as an average of 20 scans at an optimized integration time. Prior to subsequent preprocessing, all spectral curves were re-sampled with 1-nm interval. All measurements were made under clear blue-sky conditions between 10:00 and 14:00 (local time). The canopy spectra were acquired for winter wheat infected with yellow rust, powdery mildew, or aphids.

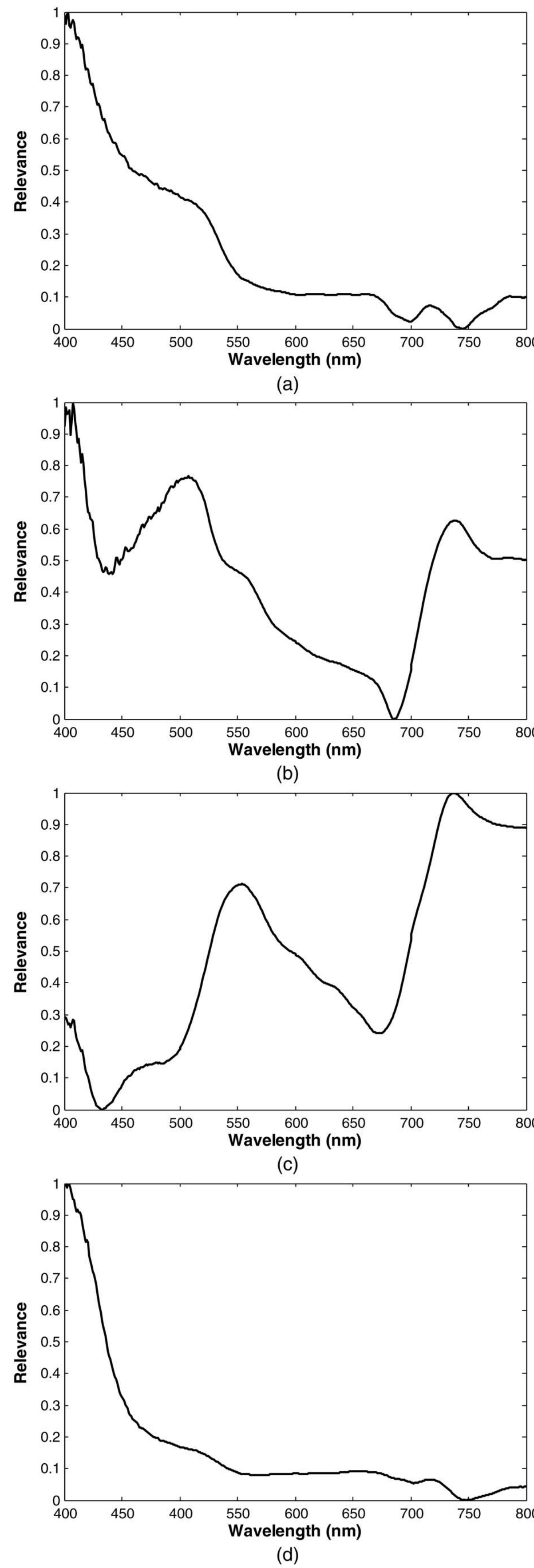

Fig. 3. Single wavelengths relevant for: (a) healthy winter wheat leaves, and (b) powdery mildew-, (c) yellow rust-, and (d) aphid-diseased winter wheat leaves, according to the RELIEF-F algorithm.

This article has been accepted for inclusion in a future issue of this journal. Content is final as presented, with the exception of pagination.

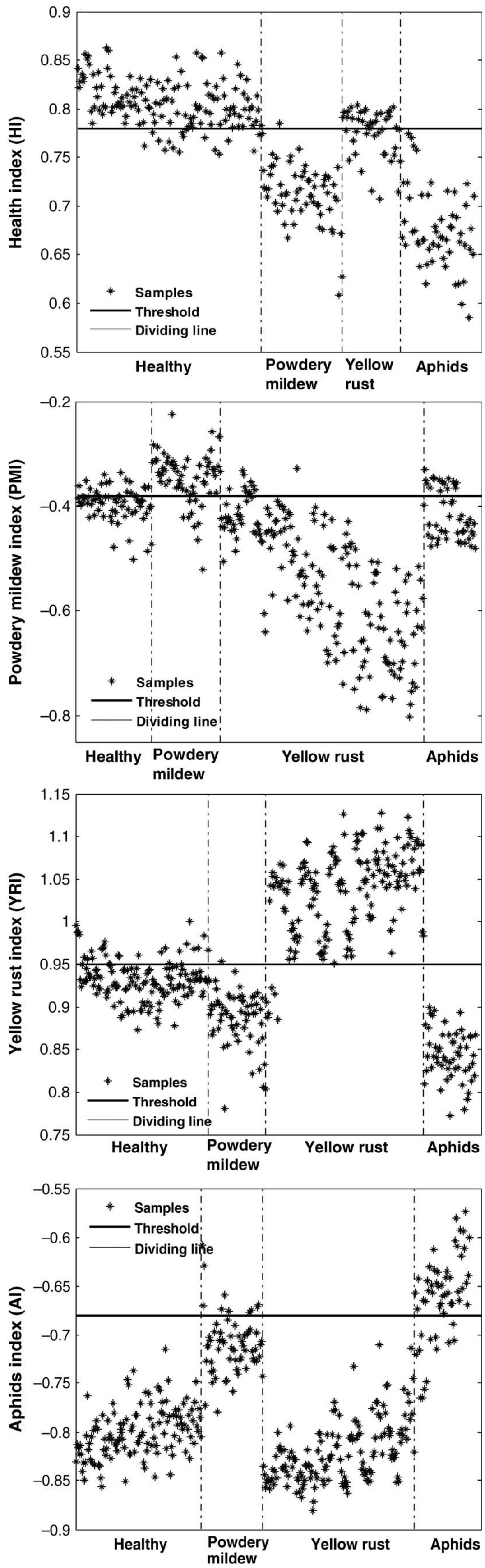

Fig. 4. Scatter plots of the classification results based on the HI, PMI, YRI, and AI.

TABLE I
CLASSIFICATION ACCURACY FOR EACH DISEASE, ACCORDING TO HI, PMI, YRI, AND AI

	Sample points	Correct points	Class accuracy(%)
HI			
All other	163	138	84.7
Healthy	141	125	88.7
Total	304	263	86.5
Kappa	0.73		
PMI			
All other	302	258	85.4
Powdery	62	52	83.9
Total	364	310	85.2
Kappa	0.57		
YRI			
All other	236	230	97.5
Yellow rust	193	163	84.5
Total	429	393	91.6
Kappa	0.83		
AI			
All other	298	288	96.7
Aphids	56	43	76.8
Total	354	331	93.5
Kappa	0.75		

H. Assessment of Disease Index

For yellow rust, the assessment of the DI was acquired at the same time as the canopy spectra were measured. To obtain the DI, 20 individual plants were randomly selected from each plot for disease inspection. When inspected, the plants were grouped into 1 of 9 classifications: 0% (incidence level, $x = 0$), 1% ($x = 1$), 10% ($x = 2$), 20% ($x = 3$), 30% ($x = 4$), 45% ($x = 5$), 60% ($x = 6$), 80% ($x = 7$), and 100% ($x = 8$) covered by rust with 0% representing no incidence of yellow rust and 100% representing the greatest incidence. The DI was then calculated using [1]

$$\mathrm{DI}(\%) = \frac{\sum (x \times f)}{n \times \sum f} \times 100 \tag{1}$$

where f is the total number of leaves of each degree of disease severity, x is the incidence level, and n is the highest incidence level (in this work, n ranged from 0 to 8).

In this study, spectra of 43 wheat leaves were measured, and the DI for each leaf was dispersed.

III. RESULTS AND ANALYSIS

A. Correlation Between Single Wavelengths

In this study, the wavelength range of 400–1000 nm was used. The correlation coefficients of different wavelengths were calculated (Fig. 2). It can be seen that closer wavelengths were highly correlated. Normalized wavelength differences describe

TABLE II
COMPARISON OF THE CLASSIFICATION ABILITY OF THE HI AND THE AI AND COMMON SPECTRAL VEGETATION INDICES: MSR, NDVI, NRI, PRI AND PHRI, SIPI, NPCI, ARI, RVSI, AND MCARI.

Index	Classification accuracy (%)	Recall		Index	Classification accuracy (%)	Recall	
		Healthy (%)	All other (%)			Aphids (%)	All other (%)
HI	86.5	88.7	84.7	AI	93.5	76.8	96.7
MSR	82.9	69.5	94.5	MSR	84.7	69.6	87.6
NDVI	83.6	71.6	93.9	NDVI	62.7	42.9	66.4
NRI	73.4	86.5	62.0	NRI	78.2	55.3	82.6
PRI	84.9	84.4	85.3	PRI	85.30	67.80	88.60
PhRI	68.4	78.0	60.1	PhRI	64.4	37.5	69.5
SIPI	72.1	92.9	53.9	SIPI	74.6	46.4	79.9
NPCI	64.8	83.7	48.5	NPCI	52.3	3.6	61.4
ARI	61.2	72.3	51.5	ARI	80.2	55.4	80.9
RVSI	78.0	88.7	68.7	RVSI	75.4	44.6	81.2
MCARI	78.3	75.2	81.0	MCARI	55.4	30.4	60.1

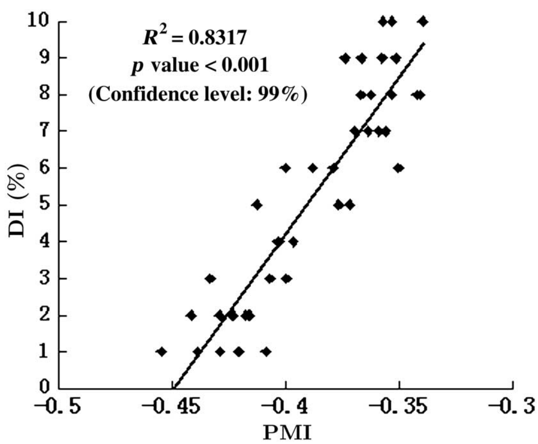

Fig. 5. Relationship between the PMI and the DI.

changes in the spectral signature, and the combination of two highly correlated wavelengths is unsuitable. Therefore, the minimal distance between wavelengths was set to 50 nm. Considering the high similarity of near infrared bands between 750 and 1000 nm (the correlation coefficients reached almost 0.9) (Fig. 2), only wavelengths ranging from 400 to 800 nm were used in the RELIEF-F algorithm.

B. NSIs of Disease

1) Construction of the Indices: Before the NSIs were established, the most relevant single wavelength for the diseases was calculated according to the RELIEF-F algorithm (Fig. 3). For healthy leaves, the most relevant single wavelengths were around 400 nm [Fig. 3(a)].

The best and worst weighted 10% of the single wavelengths were at 400 nm and between 680 and 780 nm, respectively [Fig. 3(a)]. Single wavelengths around 400, 500, and 750 nm were highly relevant for winter wheat leaves diseased with powdery mildew, and the normalized reflectance differences were around 500, 680, and 750 nm [Fig. 3(b)]. Single wavelengths relevant to yellow rust infection were around 540 and 730 nm, and for normalized reflectance differences, the wavelengths of 430 and 670 nm were included [Fig. 3(c)]. For aphid infection, the single wavelengths were around 400 nm and for normalized reflectance differences, wavelengths between 720 and 780 nm were included [Fig. 3(d)].

Single wavelengths and the normalized reflectance differences of high relevance were extracted based on the RELIEF-F algorithm, and the possible wavelength combinations and weights were calculated for the specific spectral index of each category. Finally, the health-index (HI) was derived based on reflectance at 403 nm and normalized reflectance difference between 402 and 739 nm (2). The powdery mildew-index (PMI) was proposed based on reflectance at 738 nm and normalized reflectance difference between 515 and 698 nm (3). The yellow rust-index (YRI) was calculated based on reflectance at 736 nm and normalized reflectance difference between 419 and 730 nm (4). The aphids-index (AI) was derived based on reflectance at 403 nm and normalized reflectance difference between 400 and 735 nm (5)

$$\text{Health-index (HI)}: \frac{R739 - R402}{R739 + R402} - 0.5R403 \quad (2)$$

$$\text{Powdery mildew-index (PMI)}: \frac{R515 - R698}{R515 + R698} - 0.5R738 \quad (3)$$

$$\text{Yellow rust-index (YRI)}: \frac{R730 - R419}{R730 + R419} + 0.5R736 \quad (4)$$

$$\text{Aphids-index (AI)}: \frac{R400 - R735}{R400 + R735} + 0.5R403. \quad (5)$$

2) Classification of Different Diseases: The ability of the NSIs to distinguish between diseases is shown in Fig. 4 and the classification accuracy is shown in Table I. The threshold was optimized to obtain better separation. The classification accuracies of HI, PMI, YRI, and AI were 86.5%, 85.2%, 91.6%, and 93.5%, respectively, and the Kappa indices were 0.73, 0.57, 0.83, and 0.75, respectively. These results showed that the NSIs were able to detect diseases and distinguish between them with good reliability.

3) Comparison With Common Vegetation Indices: These NSIs also had higher classification accuracy compared with other

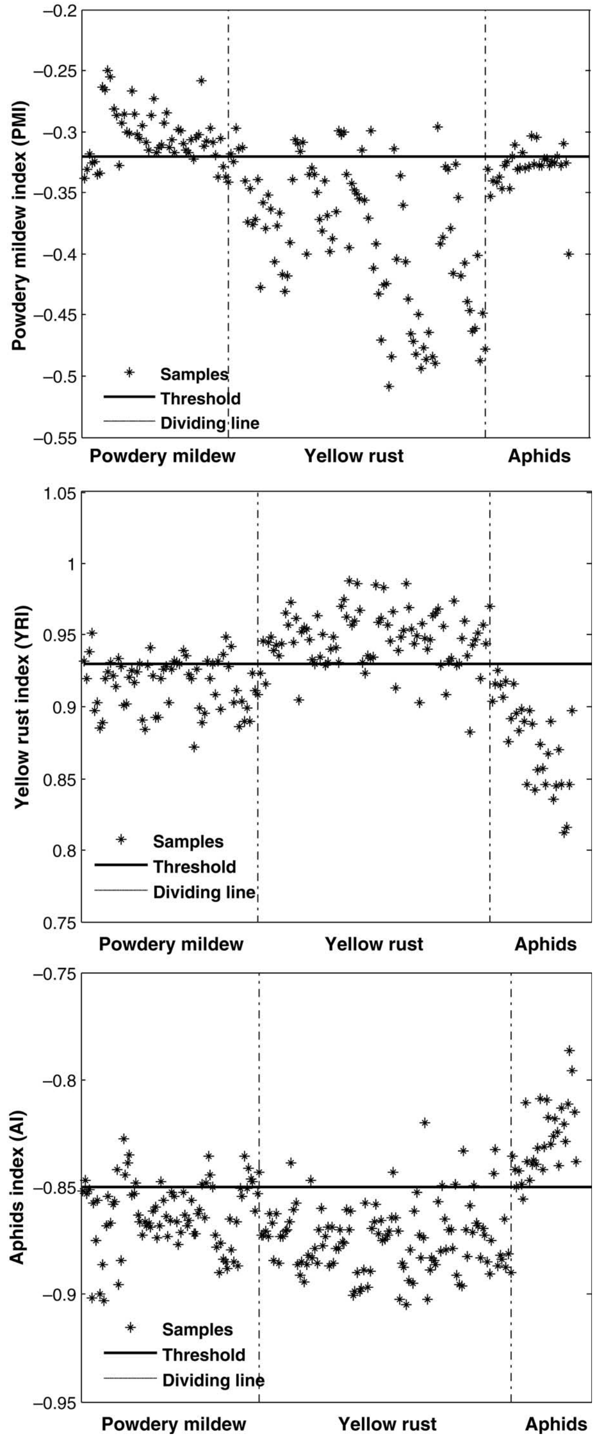

Fig. 6. Scatter plot of the classification results based on application of the PMI, YRI, and AI to canopy spectral data.

commonly used vegetation indices. The classification accuracy of the HI was the best (86.5%) for the differentiation of healthy and diseased winter wheat leaves, followed by PRI, NDVI, and MSR with classification accuracies of 84.9%, 83.6%, and 82.9%, respectively (Table II). The classification of aphid-diseased leaves was the best using AI with a classification accuracy of 93.5%. The PRI, MSR, and ARI showed acceptable classification accuracies (85.3%, 84.7%, and 80.2%, respectively). For the winter wheat, rust and powdery mildew indices were unsuitable to detect diseases with classification accuracy of 50% for all applied indices.

4) Correlation Between PMI and DI: Statistical correlation analysis was carried out on the PMI and the DI, and the DI of the remote sensing inversion model was established (Fig. 5). A significant positive correlation was found between the DI and the PMI ($R^2 = 0.83$, $n = 43$), suggesting that the PMI can potentially monitor the severity of powdery mildew.

C. Application of Spectral Disease Indices

1) Classification Based on Canopy Spectral Data: To further validate these NSIs, we used canopy spectral data of wheat infected with powdery mildew, yellow rust, and aphids. Because we had no health samples from the same period, the HI was not used for separating different diseases. The identification results of the other indices are shown in Fig. 6. The threshold needed to be recalculated for each dataset due to different experimental conditions and sensor specifications. For nonimaging data from the canopy scale, the classification accuracies of PMI, YRI, and AI were 82.4%, 84.7%, and 87.6%, respectively.

2) Estimation of the DI of Yellow Rust: For the canopy spectrum of winter wheat with yellow rust, the DI of 55 samples was measured. The YRI corresponding to the measurement sample point was calculated from the canopy data. The measured DI was divided into two parts: one for modeling and the rest for verification. Fig. 7(a) shows the scatter plot of the YRI and the DI of winter wheat. The prediction regression of the DI using the YRI can be expressed as ($n = 30$)

$$\mathrm{DI}(\%) = 1294.9\ (\mathrm{YRI}) - 1179.6(R^2 = 0.81). \qquad (6)$$

The reliability of the regression equation was satisfactory, with a regression coefficient of $R^2 = 0.81$. Fig. 7(b) shows the verification result, and the R^2 between the estimated and the measured DI was 0.86 ($n = 25$), indicating that it is feasible to use YRI to predict the severity of winter wheat diseased with yellow rust.

IV. Discussion

Different diseases can impact the spectral signature of winter wheat leaves in different ways [29]. This study showed that the NSIs offer a simple and effective way to detect diseases using hyperspectral data. Compared with the commonly used vegetation indices, the NSIs have several advantages as a result of using the RELIEF-F algorithm because this algorithm can deal with multiclass classification problems. Because the wavelengths were standardized before extraction of all NSI features, the impacts of different ecological conditions, illumination, crop type, or sensor-specific effects were reduced [30], [31]. Because the proposed NSIs are based on the combination of the most relevant wavelength and the normalized wavelength, they offer opportunities to detect and identify diseases in winter wheat using the specific characteristics of different foliar diseases.

Before identifying each disease, a binary classification needs to be carried out to separate healthy wheat plants from diseased

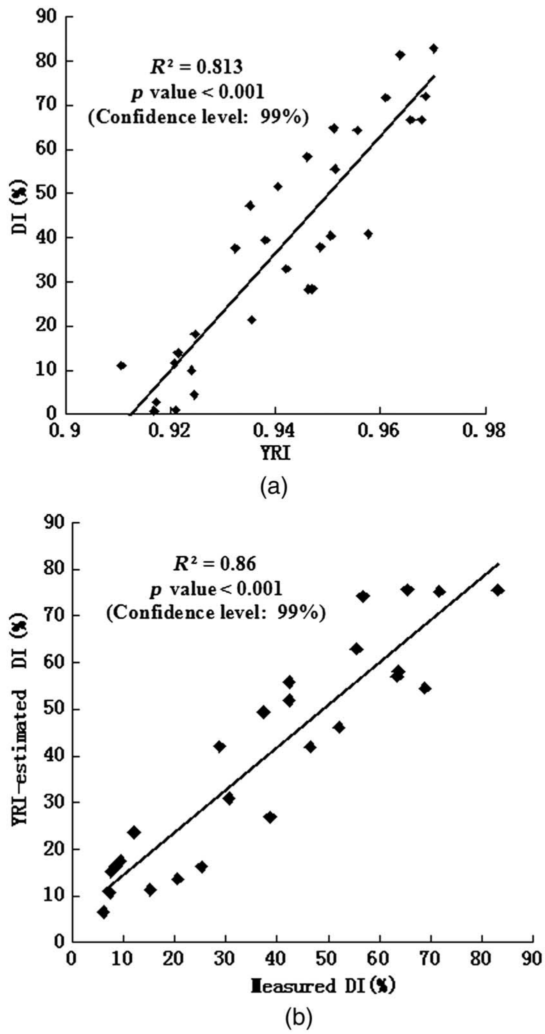

Fig. 7. YRI used to estimate the DI: (a) relationship between the measured DI and YRI and (b) relationship between the measured and YRI-estimated DI.

ones with the HI. The narrow bands that constitute the indices HI, PMI, YRI, and AI are generally centered at 400, 550, and 720 nm. As Gitelson and Merzlyak [32] indicated, the reflectance near 700 nm is a fundamental feature of green vegetation. In the past few decades, many studies have focused on plant diseases, and a large range of wavelengths in the visible and near infrared ranges have been tested [33]–[37]. For example, PMI was constituted by three narrow bands in the visible and red edge (i.e., 515, 698, and 738 nm). According to Merzlyak *et al.* [38], the reflectance from 510 to 520 nm represents the absorption maximum of carotenoids. Furthermore, the reflectance at 698 and 738 nm is close to the red-edge position [39]–[43], and migration toward the red-edge position has been used as an indicator of vegetation stress [44]–[46]. Therefore, the NSIs proposed by this study are suitable for disease detection.

The NSIs produced good results when we attempted to classify plant diseases. A successful application of datasets from the canopy scale demonstrated the transferability of these NSIs. Due to lack of data, the applicability of these NSIs for hyperspectral imaging data has not been determined. Moreover, spectral vegetation indices proposed from hyperspectral data may have more difficulty in identifying crop diseases when atmospheric conditions are poor (compared to when determined with in situ spectral measurements).

V. Conclusion

All four NSIs were able to detect and identify specific plant diseases. Using these NSIs, diseases could be identified and differentiated, which is not possible when using existing indices that are sensitive to abiotic stress conditions (i.e., indices related to chlorophyll content). We expect that the use of hyperspectral data to develop NSIs will further improve the sensitivity of disease detection in the near future. Importantly, the current analysis detected middle-stage disease in the crops, which leaves a need for discovering methods for detecting and recognizing disease in the earliest stages. Future studies should attempt to fill this gap.

Acknowledgments

The authors are grateful to Mr. W. Li, Mrs. H. Chang, and Z. Ma for data collection.

References

[1] G. B. Li, S. M. Zeng, and Z. Q. Li, *Integrated Management of Wheat Pests*. Beijing, China: Press of Agriculture Science and Technology of China, 1989.

[2] A. J. W. De Wit, H. L. Boogaard, and C. A. Van Diepen, "Spatial resolution of precipitation and radiation: The effect on regional crop yield forecasts," *Agric. Forest Meteorol.*, vol. 135, pp. 156–168, 2005.

[3] S. Sankaran, A. Mishra, R. Ehsani, and C. Davis, "A review of advanced techniques for detecting plant diseases," *Comput. Electron. Agric.*, vol. 72, pp. 1–13, 2010.

[4] S. R. Delwiche and M. S. Kim, "Hyperspectral imaging for detection of scab in wheat," *Biol. Qual. Precis. Agric.*, vol. 4203, pp. 13–20, 2000.

[5] M. Y. Huang, W. J. Huang, L. Y. Liu, Y. D. Huang, J. H. Wang, C. J. Zhao *et al.*, "Spectral reflectance feature of winter wheat single leaf infected with stripe rust and severity level inversion," *Trans. CSAE*, vol. 20, no. 1, pp. 176–180, 2004.

[6] W. J. Huang, W. L. David, Z. Niu, Y. J. Zhang, L. Y. Liu, and J. H. Wang, "Identification of yellow rust in wheat using in-situ spectral reflectance measurements and airborne hyperspectral imaging," *Precis. Agric.*, vol. 8, pp. 187–197, 2007.

[7] T. Rumpf, A. K. Mahlein, U. Steiner, E. C. Oerke, H. W. Dehne, and L. Plümer, "Early detection and classification of plant diseases with support vector machines based on hyperspectral reflectance," *Comput. Electron. Agric.*, vol. 74, no. 1, pp. 91–99, 2010.

[8] M. Mirik, R. J. Ansley, K. Steddom, D. C. Jones, C. M. Rush, G. J. Michels Jr. *et al.*, "Remote distinction of a noxious weed (musk thistle: Carduus nutans) using airborne hyperspectral imagery and the support vector machine classifier," *Remote Sens.*, vol. 5, pp. 612–630, 2013.

[9] H. H. Muhammed, "Hyperspectral crop reflectance data for characterising and estimating fungal disease severity in wheat," *Biosyst. Eng.*, vol. 91, no. 1, pp. 9–20, 2005.

[10] A. A. Gitelson, Y. J. Kaufman, R. Stark, and D. Rundquist, "Novel algorithms for remote estimation of vegetation fraction," *Remote Sens. Environ.*, vol. 80, pp. 76–87, 2002.

[11] J. Peñuelas, F. Baret, and I. Filella, "Semiempirical indices to assess carotenoids/chlorophyll a ratio from leaf spectral reflectance," *Photosynthetica*, vol. 31, pp. 221–230, 1995.

[12] A. Bannari, K. S. Khurshid, K. Staenz, and J. Schwarz, "A Comparison of Hyperspectral Chlorophyll Indices for Wheat Crop Chlorophyll Content Estimation Using Laboratory Reflectance Measurements," *IEEE Transactions on Geoscience and Remote Sensing*, vol. 45, no. 10, pp. 3063–3074, 2007.

[13] J. C. Zhang, R. L. Pu, W. J. Huang, L. Yuan, J. H. Luo, and J. H. Wang, "Using in-situ hyperspectral data for detecting and discriminating yellow rust disease from nutrient stresses," *Field Crops Res.*, vol. 134, pp. 165–174, 2012.

[14] J. W. Rouse, R. H. Haas, J. A. Schell, and D. W. Deering, "Monitoring vegetation systems in the Great Plains with ERTS," in *Proc. 3rd Earth Resour. Technol. Satell.-1 Symp.*, Greenbelt, MD, USA NASA, 1974, pp. 301–317.

[15] R. Fensholt, S. Huber, S. R. Proud, and C. Mbow, "Detecting canopy water status using shortwave infrared reflectance data from polar orbiting and geostationary platforms," *IEEE Sel. Top. Appl. Earth Observ. Remote Sens.*, vol. 3, no. 3, pp. 271–285, Sep. 2010.

[16] J. Penuelas, I. Filella, C. Biel, L. Serrano, and R. Save, "The reflectance at the 950–970 nm region as an indicator of plant water status," *Int. J. Remote Sens.*, vol. 14, no. 10, pp. 1887–1905, 1993.

[17] S. Graeff, J. Link, and W. Claupein, "Identification of powdery mildew (*Erysiphe graminis* sp. tritici) and take-all disease (*Gaeumannomyces graminis* sp. tritici) in wheat (*Triticum aestivum* L.) by means of leaf reflectance measurements," *Cent. Eur. J. Biol.*, vol. 1, pp. 275–288, 2006.

[18] E. Luedeling, A. Hale, M. Zhang, W. J. Bentley, and L. C. Dharmasri, "Remote sensing of spider mite damage in California peach orchards," *Int. J. Appl. Earth Observ. Geoinf.*, vol. 11, pp. 244–255, 2009.

[19] A. K. Mahlein, T. Rumpf, P. Welke, H. W. Dehne, L. Plümer, U. Steiner *et al.*, "Development of spectral indices for detecting and identifying plant diseases," *Remote Sens. Environ.*, vol. 128, pp. 21–30, 2013.

[20] M. Robnik-Šikonja and I. Kononenko, "Theoretical and empirical analysis of ReliefF and RreliefF," *Mach. Learn.*, vol. 53, no. 1, pp. 23–69, 2003.

[21] K. Kira and L. Rendell, "A practical approach to feature selection," in *Proc. 9th Int. Workshop Mach. Learn.*, San Mateo, CA, USA Morgan Kaufmann Publishers Inc., 1992, pp. 249–256

[22] J. M. Chen, "Evaluation of vegetation indices and a modified simple ratio for boreal applications," *Can. J. Remote Sens.*, vol. 22, pp. 229–242, 1996.

[23] I. Filella, L. Serrano, J. Serra, and J. Penuelas, "Evaluating wheat nitrogen status with canopy reflectance indices and discriminant analysis," *Crop Sci.*, vol. 35, pp. 1400–1405, 1995.

[24] J. A. Gamon, J. Peñeulas, and C. B. Field, "A narrow-waveband spectral index that tracks diurnal changes in photosynthetic efficiency," *Remote Sens. Environ.*, vol. 41, pp. 35–44, 1992.

[25] J. Peñuelas, J. A. Gamon, A. L. Fredeen, J. Merino, and C. B. Field, "Reflectance indices associated with physiological changes in nitrogen- and water-limited sunflower leaves," *Remote Sens. Environ.*, vol. 48, pp. 135–146, 1994.

[26] A. A. Gitelson, N. M. Merzlyak, and B. O. Chivkunova, "Optical properties and nondestructive estimation of anthocyanin content in plant leaves," *Photochem. Photobiol.*, vol. 74, pp. 38–45, 2001.

[27] R. Merton and J. Huntington, "Early simulation of the ARIES-1 satellite sensor for multi-temporal vegetation research derived from AVIRIS," in *Proc. Summ. 8th JPL Airborne Earth Sci. Workshop*, Pasadena, CA, USA JPL Publication, 1999, pp. 299–307.

[28] C. S. Daughtry, C. L. Walthall, M. S. Kim, E. B. de Colstoun, and J. E. McMurtrey, "Estimating corn leaf chlorophyll concentration from leaf and canopy reflectance," *Remote Sens. Environ.*, vol. 74, pp. 229–239, 2000.

[29] C. J. Cai, Z. H. Ma, H. G. Wang, Y. P. Zhang, and W. J. Huang, "Comparison research of hyperspectral properties between near-ground and high altitude of wheat stripe rust," *Acta Phytopatholog. Sin.*, vol. 37, pp. 77–82, 2007.

[30] T. M. Lillesand and R. W. Kiefer, *Remote Sensing and Image Interpretation*, New York, NY, USA: Wiley, 2000.

[31] J. Lyon, D. Yuan, R. Lunetta, and C. Elvidge, "A change detection experiment using vegetation indices," *Photogramm. Eng. Remote Sens.*, vol. 64, no. 2, pp. 143–150, 1998.

[32] A. A. Gitelson and M. N. Merzlyak, "Remote estimation of chlorophyll content in higher plant leaves," *J. Plant Physiol.*, vol. 148, pp. 494–500, 1996.

[33] J. R. Thomas and H. W. Gausman, "Leaf reflectance vs. leaf chlorophyll and carotenoid concentrations for eight crops," *Agron. J.*, vol. 69, pp. 799–802, 1977.

[34] C. Buschmann and E. Nagel, "In vivo spectroscopy and internal optics of leaves as basis for remote sensing of vegetation," *Int. J. Remote Sens*, vol. 14, pp. 711–722, 1993.

[35] C. Bravo, D. Moshou, J. West, A. McCartney, and H. Ramon, "Early disease detection in wheat fields using spectral reflectance," *Biosyst. Eng.*, vol. 84, pp. 137–145, 2003.

[36] D. Moshou, C. Bravo, J. West, S. Wahlen, A. McCartney, and H. Ramon, "Automatic detection of 'yellow rust' in wheat using reflectance measurements and neural networks," *Comput. Electron. Agric.*, vol. 44, pp. 173–188, 2004.

[37] R. Devadas, D. W. Lamb, S. Simpfendorfer, and D. Backhouse, "Evaluating ten spectral vegetation indices for identifying rust infection in individual wheat leaves," *Precis. Agric.*, vol. 10, pp. 459–470, 2009.

[38] M. N. Merzlyak, A. A. Gitelson, O. B. Chivkunova, and V. Y. Rakitin, "Non-destructive optical detection of pigment changes during leaf senescence and fruit ripening," *Physiol. Plant.*, vol. 106, pp. 135–141, 1999.

[39] D. N. H. Horler, M. Dockray, and J. Barber, "The red edge of plant leaf reflectance," *Int. J. Remote Sens.*, vol. 4, no. 2, pp. 273–288, 1983.

[40] F. Boochs, G. Kupfer, K. Dockter, and W. Kuhbauch, "Shape of the red-edge as vitality indicator for plants," *Int. J. Remote Sens.*, vol. 11, no. 10, pp. 1741–1753, 1990.

[41] J. G. P. W. Clevers, S. M. Jong, G. F. Epema, F. D. Meer, W. H. Bakker, A. K. Skidmore, *et al.*, "Derivation of the red edge index using MERIS standard band setting," *Int. J. Remote Sens.*, vol. 23, no. 16, pp. 3169–3184, 2002.

[42] W. Collins, G. L. Raines, and F. C. Canney, "Airborne spectroradiometer discrimination of vegetation anomalies over sulphide mineralisation—A remote sensing technique," in *Abstract with Programmes*, Seattle, Washington, USA Geological Society of America, Nov. 7–9, 1977, pp. 932–933.

[43] C. Y. Wu, Z. Niu, Q. Tang, and W. J. Huang, "Estimating chlorophyll content from hyperspectral vegetation indices: Modeling and validation," *Agric. Forest Meteorol.*, vol. 148, pp. 1230–1241, 2008.

[44] P. J. Curran, W. R. Windham, and H. L. Gholz, "Exploring the relationship between reflectance red edge and chlorophyll concentration in slash pine leaves," *Tree Physiol.*, vol. 15, pp. 203–206, 1995.

[45] D. W. Lamb, M. Steyn-Ross, P. Schaare, M. M. Hanna, W. Silvester, and A. Steyn-Ross, "Estimating leaf nitrogen concentration in ryegrass (*Lolium* spp.) pasture using the chlorophyll red-edge: Theoretical modelling and experimental observations," *Int. J. Remote Sens.*, vol. 23, no. 18, pp. 3619–3648, 2002.

[46] K. L. Smith, M. D. Steven, and J. J. Colls, "Use of hyperspectral derivative ratios in the red edge region to identify plant stress responses to gas leak," *Remote Sens. Environ.*, vol. 92, pp. 207–217, 2004.

Wenjiang Huang received the Ph.D. degree in cartography and geographic information society (GIS) from Beijing Normal University, Beijing, China, in 2005.

He is currently with the Key Laboratory of Digital Earth Science, Institute of Remote Sensing and Digital Earth, Chinese Academy of Sciences, Beijing, China. His current research interests include quantitative remote sensing application in vegetation monitoring and application and the digital earth science.

Qingsong Guan received the B.C. degree from Anhui University, China, in 2011, where he is currently a graduate student.

His current research interests include quantitative remote sensing application in agriculture and agricultural disease and pest detection.

Juhua Luo received the Ph.D. degree in cartography and GIS from Beijing Normal University, Beijing, China, in 2012.

She is currently with State Key Laboratory of Lake Science and Environment, Nanjing Institute of Geography and Limnology, Chinese Academy of Sciences, Nanjing, China. Her current research interests include remote sensing and GIS applications in hyperspectral analyzing, agricultural disease and pest detection, and subaquatic plant monitoring by remote sensing.

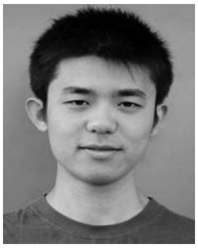

Jingcheng Zhang received the Ph.D. degree in agricultural remote sensing and information technology from Zhejiang University, Hangzhou, China, in 2012.

He is currently with Beijing Research Center for Information Technology in Agriculture, Beijing, China. His current research interests include hyperspectral analyzing, agricultural disease detection, and monitoring by incorporating multi-sources of remote sensing data.

Jinling Zhao received the Ph.D. degree in cartography and GIS from the Institute of Geographic Sciences and Natural Resources Research, Chinese Academy of Sciences (CAS), Beijing, China, in 2010.

He is currently with Key Laboratory of Intelligent Computing and Signal Processing, Ministry of Education, Anhui University, Hefei, China. His current research interests include remote sensing and GIS applications in land-use and land-cover change (LUCC), agricultural disasters.

Dong Liang received the Ph.D. degree in circuits and systems from Anhui University, Hefei, China, in 2002.

He is currently with the Key Laboratory of Intelligent Computing and Signal Processing, Ministry of Education, Anhui University, Hefei, China. His research field includes image processing, computing signal processing, and pattern recognition.

Linsheng Huang received the Ph.D. degree in circuits and systems from Anhui University, Hefei, China, in 2013.

He is currently with the Key Laboratory of Intelligent Computing and Signal Processing, Ministry of Education, Anhui University, Hefei, China. His current research interests include remote sensing image processing, technology, and applications of vegetation.

Dongyan Zhang received the Ph. D. degrees from Zhe Jiang University, China, in 2012. His major subject is agricultural remote sensing and information technology.

His research interests concentrate in computer image processing, hyperspectral remote sensing, and sensors applying in agriculture and environment.